Chin.J.Geochem.(2012)31:030–040
DOI: 10.1007/s11631-012-0546-6

Radioactivity and mineralogy of the altered granites of the Wadi Ghadir shear zone, South Eastern Desert, Egypt

Mohamed F. Raslan* and Mohamed G. El-Feky
Nuclear Materials Authority, El Maadi P.O. Box 530, Cairo, Egypt
** Corresponding author, E-mail: raslangains@hotmail.com*

Received June 29, 2010; accepted July 30, 2010

Abstract Quartz-diorite, gneissose granodiorites, two-mica granite and perthite leucogranie are the main rock units cropping out in the Wadi Ghadir area, South Eastern Desert of Egypt. Along the NNE-SSW mega-faults, a broad brittle shear zone is developed in the Ghadir two-mica granite. Brittle deformation is manifested by severe mylonitization and alteration of these granites. These sheared altered granites are characterized by the presence of radioactive mineralization, associated with alteration features such as silicification, hematization and kaolinitization.

Radioelement measurements revealed that the unaltered and altered two-mica granites are considered as uraniferous granites. The average uranium and thorium contents in the unaltered two-mica granites are 12.29×10^{-6} and 19.81×10^{-6}, respectively, and the average Th/U ratio is 1.62. The altered granites exhibit higher concentrations of U (averaging 97.949), but have lower Th and Th/U ratios (13.83 and 0.16, respectively), which indicates uranium enrichment in the granites. Binary relations of eTh/eU against either eU or eTh and eU with eTh in the studied granites suggest that the distribution of radioactive elements not only magmatic (positive correlation between eU and eTh), but also due to hydrothermal redistribution of radioelements (weak correlation between eU and eTh/eU).

The magmatic U and Th are indicated by the presence of uraninite, thorite, zircon and monazite whereas the evidence of hydrothermal mineralization is the alteration of rock-forming minerals such as feldspar and the formation of secondary minerals such as uranophane and pyrite.

Microscopic, XRD and scanning electron microscopic studies revealed the presence of uraninite, uranophane, thorite, Ce-monazite and zircon, in addition to phlogopite-fluor mica in the studied altered granites of the Wadi Ghadir shear zone.

Key words granite; radioelement measurement; uraninite; uranophane; thorite; Ce-monazite; zircon; Wadi Ghadir

1 Introduction

The uranium occurrences in Egypt are associated with Gabal Qattar, Gabal El Missikat, Gabal Um Ara and Gabal El Sella (Roz, 1994; Abu Dief, 1985; Ibrahim, 1986; Assaf et al., 1996). Most of these granitic occurrences are mainly subalkaline (biotite only or biotite and amphibole), also called high-K calc-alkaline or transalkaline granites, sometimes with secondary muscovite, developed during late- to post-magmatic hydrothermal alteration. Few peraluminous two-mica granites in Egypt are associated with visible U-mineralization, e.g. Gabal El Sella (Assaf et al., 1996; Ibrahim et al., 2001).

The study area has been described by several authors, e.g. Sabet et al. (1978), El-Sharkawy and El-Bayoumi (1979). El-Sharkawy and El-Bayoumi (1979) classified the rocks cropping out along the eastern part of Wadi Ghadir as granites belonging to the older and younger (Gattarian) granites. Takla et al. (1992) classified the granitoids of Wadi Ghadir as (a) diorites and granodiorites that are similar in their characteristics to the older granites and (b) younger granites that have the characteristics similar to those of alkalic and other anorogenic granitic suits. Ibrahim and Ali (2003) reported the presence of secondary uranium mineralization (uranophane) in the study area. The main target of this work is to shed light on the radioactive mineralization of the altered granites of the Wadi Ghadir shear zone.

2 Geological setting

The studied granitoid rocks at Wadi Ghadir cover

an area about of 39.6 km^2 and are differentiated into the older granites (quartz diorite and gneissose granodiorite) and younger granites (two-mica granite and perthitic-leucogranite) (Fig. 1A). Quartz diorite rocks cover an area of about 16.7 km^2 in the northwestern half of the map area (Fig. 1A). They are intruded by perthitic leucogranite with sharp intrusive contacts. The quartz diorite is composed of plagioclase, hornblende, quartz, biotite and orthoclase. Zircon, apatite, sphene and opaques are the main accessory minerals. Gneissose granodiorite rocks cover an area of about 14 km^2 (Fig. 1A) in the southeastern part of the map area. They occupy a high terrain and intrude the younger granites with sharp intrusive contacts. They enclose elongated amphibolite xenoliths and are invaded by dykes of different compositions ranging from aplite, felsite to basalt. The rocks are composed of plagioclase, quartz, potash feldspars, biotite and hornblende. zircon, epidote, apatite, sphene and opaques are the main accessory minerals (Ibrahim and Ali, 2003).

The younger granites are classified as two-mica granite and perthitic leucogranite of monzogranite and synogranite composition, respectively (Fig. 1A). The two-mica granite is medium- to coarse-grained and whitish- to reddish-pink in color. It covers an area of about 2.3 km^2 in the central-eastern part of the map area (Fig. 1A). It is intruded into the gneissose granodiorite with intrusive sharp contacts and invaded by quartz veins. Silicification, hematization and kaolinitization as well as the development of spotty or dendrite manganese oxides along the fracture planes are the most pronounced post-magmatic hydrothermal alteration characteristics of these rocks. High intensity of radioactivity occurs mainly in association with these types of alterations. The rock is composed of potash feldspar, quartz, plagioclase, biotite and muscovite. Zircon, apatite, monazite, sphene and opaques are the main accessory minerals.

Perthitic leucogranite is medium- to coarse-grained. It occupies an area of about 6.6 km^2, elongated in a NW-SE direction and parallel to the regional structure (Fig. 1A). It is pink to reddish-pink in color and characterized by blocky and exfoliation weathering. It is fractured in different directions. Silicification, hematization and development of Mn-dendrites along fracture planes represent the post-magmatic hydrothermal alteration features. The rock is composed of potash feldspar, quartz, plagioclase and minor amounts of biotite. Zircon, fluorite, apatite, sphene and opaques are the main accessory minerals.

Shear zone and wall-rock alteration

The initial identification of these shear zones was based on landsat images and field observations. The shear zone of the Ghadir two-mica granite is located at the southeastern segment of the studied granites, and extends for 0.5 km. The NNE-SSW sets of faults cut through most of the granitic plutons. These faults are mainly of the strike-slip type (sinistral) and vary in length from 0.5 to 4 km. The granite becomes cataclased and sheared within the shear zone. The intensely mineralized part (highly radioactive) of the shear zone varies in width from 0.2 to 2 m and in length from 50 to 100 m (Fig. 1B and C).

Ferrugination and kaolinization with a few dark patches of manganese oxide are the main wall-rock alterations. These alterations of granite are more pronounced on both sides of the shear zone. The deep reddish-brown color mostly features the strongly mineralized lenses of iron and manganese oxides, while the lighter tones in the sheared granites such as greasy and brownish-yellow colors could be attributed to the destruction of feldspars by kaolinization process.

In the past no detailed study has been carried out on the shear zone in the two-mica granite of the Wadi Ghadir area.

3 Sampling and analytical techniques

Representative grab samples were collected from the two-mica granite (seven samples) and from the altered granites of the Wadi Ghadir shear zone (fourteen samples), to represent the highest values of anomalous field radioactivity. These samples were prepared for gamma-ray spectrometric analysis in order to determine their uranium, thorium, radium and potassium contents by using a multichanel analyzer equipped with a γ-ray detector (Gamma-Spectrometer technique). The instrument used in determination of the four radioactive elements consists of a bicron scintillation detector NaI (Tl) 76×76 mm, hermetically sealed with the photomultiplier tube in aluminum housing. The tube is protected by a copper cylinder measured at 0.6 cm in thickness against induced X-ray and a chamber of lead bricks against environmental radiation. Uranium, thorium, radium and potassium are measured by using four energy regions representing Th-234, Pb-212, Pb-214 and K-40 at 93, 239, 352 and 1460 kV for uranium, thorium, radium and potassium, respectively. The measurements were carried out in plastic sample containers, cylindrical in shape, 212.6 cm^3 in volume, 9.5 cm in average diameter and 3 cm in height. The rock sample was crushed as fine as about 1 mm in grain size, and then the container was filled with about 300–400 gm of the crushed sample, sealed well and left for at least 21 days to accumulate free radon to attain radioactive equilibrium. The relation between the percentage of Rn-222 accumulation and time increased till reaching the steady stage in about 38 days (Matolin, 1991).

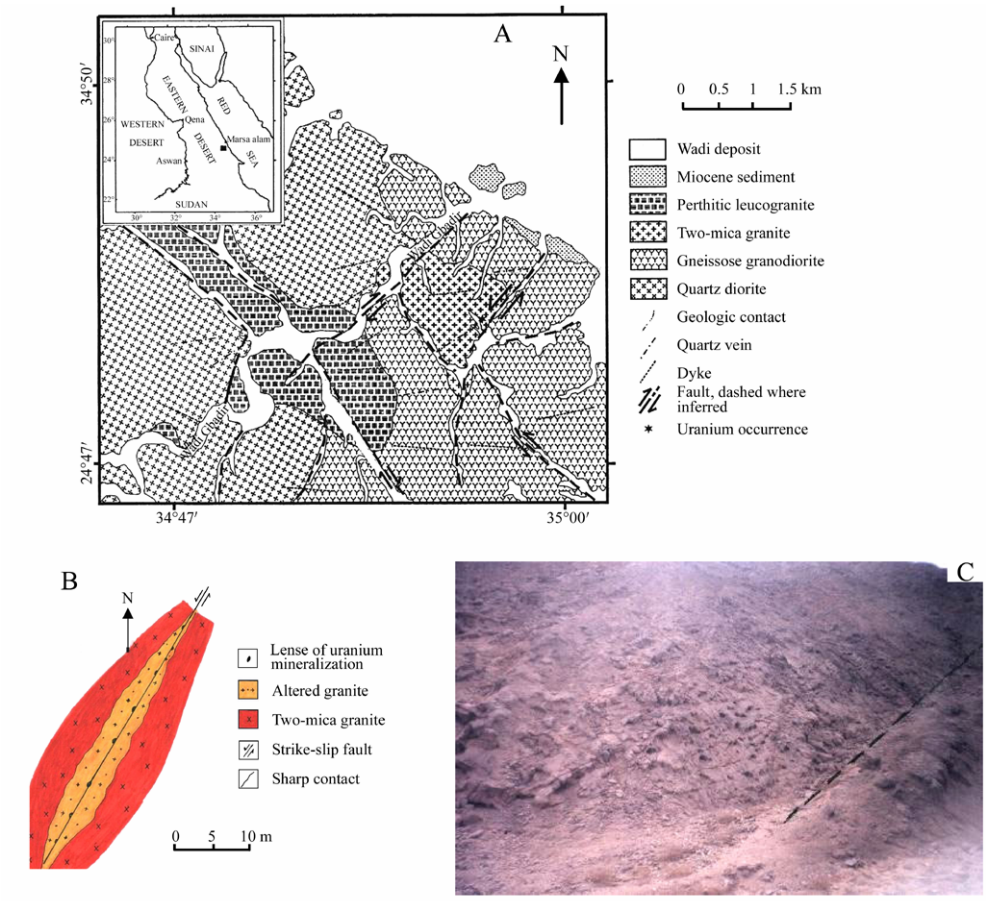

Fig. 1. A. Geological map of the Wadi Ghadir area, South Eastern Desert. Modified from Takla et al. (1992); B. sketch showing the studied shear zone in the Wadi Ghadir granites; C. mineralized shear zone (N 15° E) of the two-mica granites at Wadi Ghadir. Note: The sheared granites on the fault zone.

Also, polished thin-sections of some altered rock samples were prepared for petrographic investigation. In addition, a large bulk composite sample representing the altered mineralized granite was collected for mineralogical investigation. The sample was properly crushed, ground and sieved before subjecting the liberated-size fractions to heavy mineral separation with bromoform (Sp. Gr.=2.85 gm/cm^3). From the obtained heavy fractions, pure mineral grains were hand-picked and investigated under the binocular microscope. Some of the picked mineral grains were subjected to X-ray diffraction analysis with a Phillips X-ray diffractometer (Model PW-105018) and an Environmental Scanning Electron Microscope (ESEM). This instrument is supported by an energy dispersive spectrometer unit (EDS) (model Philips XL 30). The applied analytical conditions are: accelerating voltage 30 kV, beam diameter 1–2 μm during 60 to 120 seconds as the counting time and minimum detectable weight concentration from 0.1 wt% to 1 wt%. All these analyses were carried out at the laboratories of the Egyptian Nuclear Materials Authority (NMA).

Petrography of the altered two-mica granite

Altered granites show deformation textures with pronounced lineation and foliation, but in some cases their igneous textures are still preserved. The rock consists of potash feldspar, quartz, plagioclase, biotite and muscovite. Kaolinite, chlorite and epidote are the secondary minerals. The accessories are mainly metamict zircon, monazite, fluorite, magnetite and pyrite. Rock constituents are highly mylonitized due to brittle deformation resulting from severe deformation (Fig. 2A). Alkali feldspars are represented by string- and patchy-type perthite with subordinate microcline. They are kaolinized along cleavage planes and fractures and penetrated by relatively fine-grained veinlets of quartz. Quartz shows clear signs of strong mylonitization and deformation with its crystals displaying anhedral ropy shaped and wavy extinction (Fig. 2B). Also, quartz sometimes intergrows with K-feldspar, forming graphic texture (Fig. 2C). The cracks in perthites and mylonitized quartz promoted the movement of late iron-rich hydrothermal solutions,

which caused iron staining and gave the rock its red coloration. Uranophane occurs as fracture fillings associated with disseminated crystals of uraninite and iron oxides (Fig. 2D, E). Albite (10%) is commonly altered to sericite and the abundance of sericite increases in the mineralized samples. Cataclasis may produce microcracks in the feldspar crystals and cause winding of their twin lamellae. Biotite is a common mafic mineral in these granites. It occurs in flakes of variable sizes and shapes. Muscovite occurs as irregular flakes in the interstitial space between quartz and feldspar. It appears to be squeezed and deformed due to secondary growth of feldspar and quartz crystals. The extensive sericitization of feldspars and chloritization of biotite may support a later hydrothermal effect on this rock. The study of thin-polished sections (in reflected light) indicated that pyrite is the main sulfide mineral (Fig. 2F). Iron oxides are observed in all studied sections, both the primary-phase (magnetite) (Fig. 2G) and the secondary one resulting from the alteration of primary iron minerals which disappeared completely and pseudomorphed by hematite to limonite.

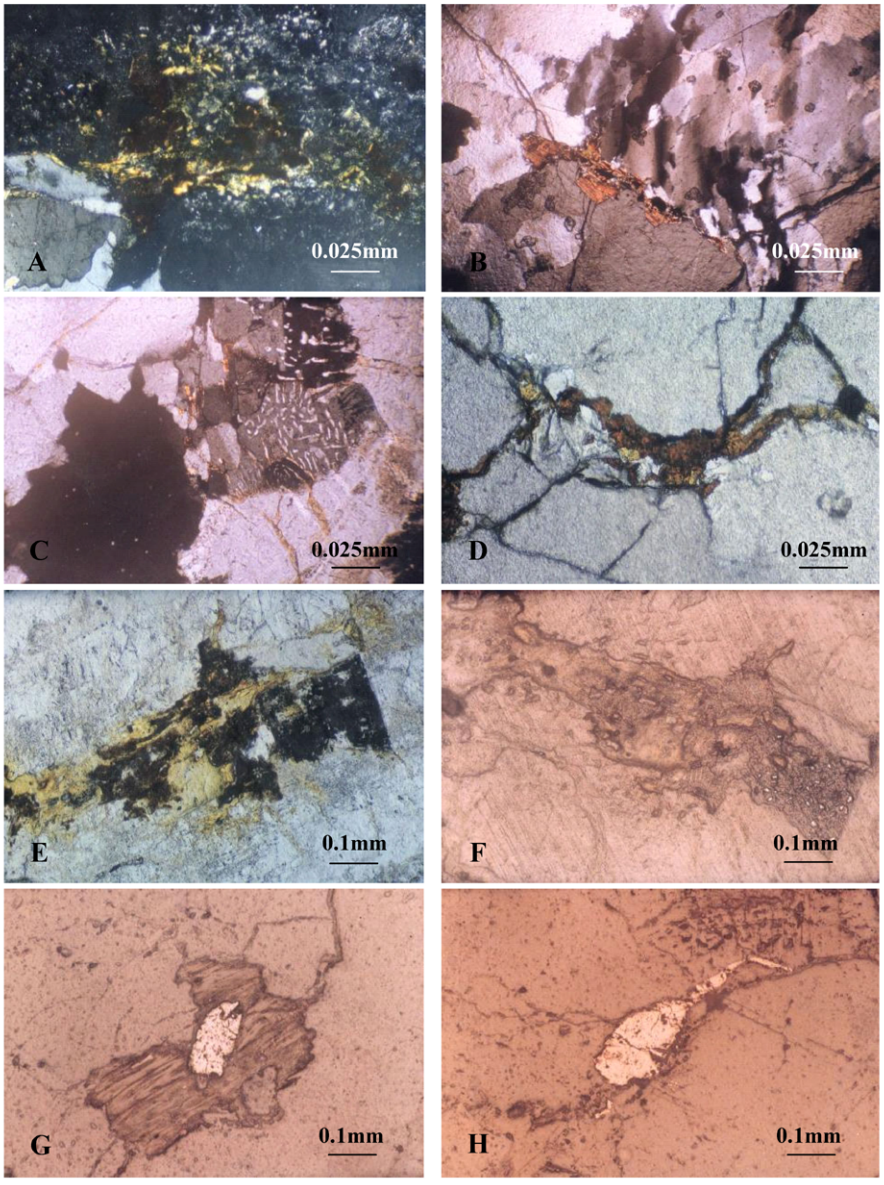

Fig. 2A. Mylonite texture in altered granites, in crossed nicols, C.N.; B. wavy extinction of foliated quartz in altered granites, in crossed nicols, C.N.; C. micrographic texture in altered granites, in crossed nicols, C.N.; D. fracture filled with uranophane and opaques, in crossed nicols, C.N.; E. secondary uranium minerals (uranophane) resulting from the alteration of primary minerals (uraninite), in polarized light, P.L.; F. disseminated minute crystals of uraninite, reflected light, R.L.; G. subhedral pyrite grains enclosed in biotite crystals, reflected light, R.L.; H. magnetite grains associated with the fractures of iron oxides, reflected light, R.L.

4 Radioactive inspection

Two-mica granites and their sheared variety (altered granites) have high U contents. U contents range from (6.61–18.52)×10^{-6} in the two-mica granites and from (38.29–225)×10^{-6} in the altered granites. They are considered as the uraniferous granites according to Darnely (1982) and Assaf et al. (1997), who defined the uraniferous granites as the granites which contain at least twice the Clark value of uranium (4×10^{-6}) (Clark et al., 1966). The granites may be or not be associated with uranium mineralization. The high uranium contents and low Th/U ratios also reflect the uraniferous nature of the studied granites. In addition to that, the altered granites can be classified as minarlized granites, which contain different types of radioactive minerals such as uranophane and uraninete.

The geochemistry of U and Uh during magmatic differentiation has been studied in many types of granites from different areas. Generally, during magmatic differentiation, the Th/U ratio remains constant. Rogers and Adams (1969) suggested 3.5 to 4 for the Th/U ratios in the granites. These ratios can either increase (Whitfield et al., 1959; Rogers and Ragland, 1961) or decrease (Larsen and Gottfried, 1960), depending on the redox conditions, the volatile contents, or alterations by endogen or supergene solutions (Falkum and Rose-Hansen, 1978). Typical eTh/eU ratios in igneous rocks are 3:1 or 4:1 whereas Th/U ratios of the two-mica granites and altered granites are 1.62 and 0.16 on average, respectively. eU-eTh variation diagram of the studied granitic rocks reflects a moderately positive correlation, which indicates that magmatic processes played an important role in the concentration of radioelements (Fig. 3A). eTh/eU ratios are directly positively correlated with thorium and defined to be weakly correlated with uranium in the two-mica and altered granites, respectively, which suggests that the distribution of radioactive elements not only magmatic but also due to hydrothermal redistribution of radioelements (Fig. 3B, C).

Cuney et al. (1984) defined the fertile granites as the highly differentiated peraluminous two-mica granites, which are characterized by high silica and uranium contents (more than 73% and 8×10^{-6}, respectively). Two-mica granites in the Wadi Ghadir area were previously chemically analyzed by Ibrahim and Ali (2003) and it was demonstrated that SiO_2 contents range from 71.60 to 73.80, in addition to the observed high uranium contents, suggesting their fertility.

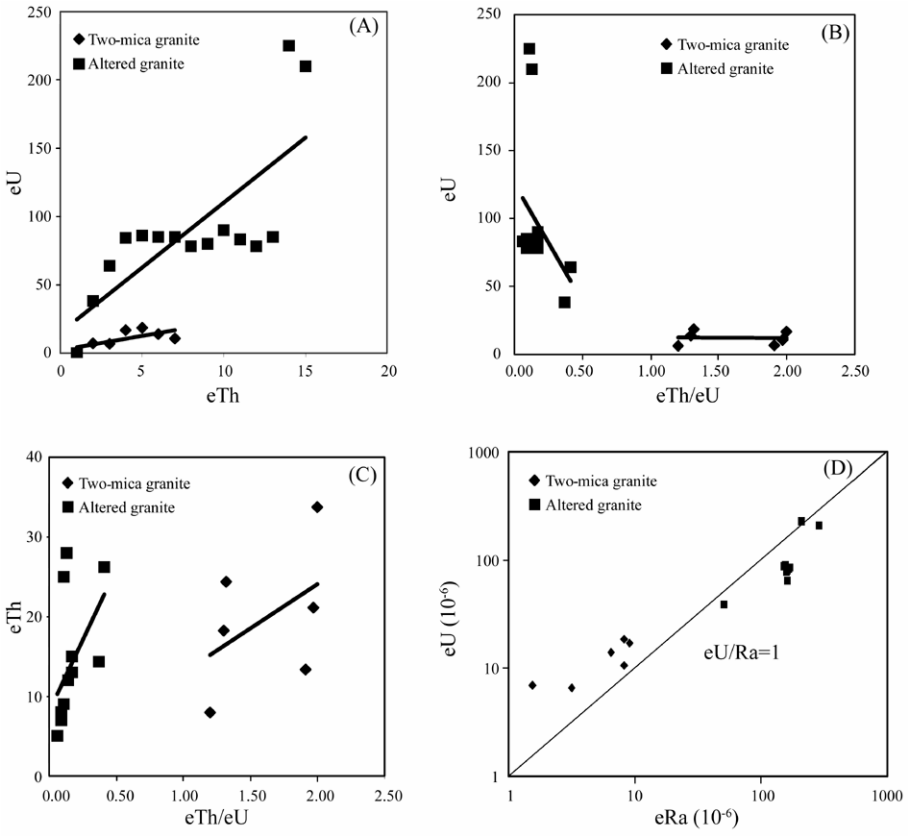

Fig. 3. Binary diagrams showing (A) eU vs. eTh, (B) eU vs. eTh/eU, (C) eTh vs. eTh/eU and (D) eU vs. Ra.

Yanting et al. (1982) used some statistical parameters e.g. X (average content), S (standard deviation) and C.V. (coefficient of variation) based on 29 granitic massifs in eastern Guangdong Province, China, to classify granitoids on the radioactive basis. According to the work of Yanting et al. (1982), four essential groups of U dispersion are defined.

Group I: average uranium content (X), standard variation (S) and coefficient of variation (C.V) are all relatively low. The lithology determines the uranium distribution. Uranium is largely syngenetic and is of rather uniform distribution. In eastern Guangdong Province, this group is mainly represented by granodiorites, and a few by monzo-granites and biotite-granites. These rock massifs are not favorable for uranium mineralization and it is difficult to find any anomaly in them.

Group II: X is high, and C.V is low. The uranium contents of these rocks show that the rocks are syngenetic, but they are not favorable for mineralization, because of missing late remobilization. In eastern Guangdong, most of the massifs belonging to this group are granites and a few are monzo-granites.

Group III: X is low; S and C.V are higher. This kind of rocks, especially granites, is in possession of high values of C.V., because the original petrochemistry of the rock massifs is either changeable or transformed. No mineralization has been discovered so far in this kind of rocks.

Group IV: X, S and C.V are all high. The granitic massifs in this group are mainly biotite-granites or two-mica granites, and these rocks are considered to be favorable for uranium mineralization. Accordingly, the Ghadir two-mica granites and their altered varieties are affiliated to Group IV because of their high X, S and C.V., i.e., the uraniferous granitoids (Table 2). On the same basis, Mahdy (1998) and El-Feky (2000) reported the same results for the Gattarian and Hangaliya granites, respectively.

Radioactive equilibrium

According to Reeves and Brooks (1978), uranium (^{238}U series) attained the equilibrium state in nearly 1.5 Ma. Cathelineau (1987) stated that uranium mineralization is affected by different processes. Leaching, mobility and redistribution of uranium are affected by hydrothermal solutions and/or supergene fluids, which cause disequilibrium in the radioactive decay series in the U-bearing rocks. The radioactive equilibrium of the studied granitic rocks can be determined by the calculation of equilibrium factor (P) which is the ratio of radiometric uranium content (eU) to radium content Ra(eU); P_{factor}=eU/Ra(eU) (Hussein, 1978; El-Galy, 1998; Surour et al., 2001).

The P_{factor} of the studied two-mica granites is more than one (2.35) (Table 1 and Fig. 3D), indicating disequilibrium in U-decay due to the addition of uranium in these rocks. On the other hand, the altered granites are also in disequilibrium state, where this average amounts to 0.58, suggesting leaching for uranium (Table 1 and Fig. 3D). From the previous discussions and relationships, it can be concluded that the magmatic differentiation played an important role in uranium enrichment in the accessory minerals, but the post-magmatic processes also played a very important role in concentrating uranium along fractures, joints and fault planes.

Table 1 Radioelement measurements for two-mica and altered granites

Rock type	Sample No.	eU0 ($\times10^{-6}$)	eTh ($\times10^{-6}$)	eRa ($\times10^{-6}$)	K (%)	eTh/eU	eU/Ra
Two-mica granite	1	6.97	13.34	1.56	3.39	1.91	4.47
	2	6.61	7.95	3.20	0.26	1.20	2.07
	3	16.86	33.75	9.15	0.11	2.00	1.84
	4	18.52	24.40	8.22	2.27	1.32	2.25
	5	14.07	18.26	6.46	1.60	1.29	2.18
	7	10.7	21.13	8.28	3.77	1.97	1.29
Altered granite	AN2	38.29	14.35	51.86	3.78	0.37	0.74
	AN1	64	26.22	165	3.26	0.41	0.39
	1S	84	12	161	3.04	0.14	0.52
	2S	86	15	153	3.33	0.17	0.56
	3S	85	8	170	3.55	0.09	0.50
	4S	85	9	165	4.09	0.10	0.52
	5S	78	13	161	3.24	0.17	0.48
	11	80	7	165	2.79	0.09	0.48
	12	90	15	156	2.84	0.17	0.58
	13	83	5	166	2.57	0.06	0.50
	14	78	7	161	3.12	0.09	0.48
	15	85	9	164	2.98	0.11	0.52
	A1	225	25	210	4.61	0.15	1.07
	A2	210	28	293	5.07	0.13	0.72

Table 2 Summary of the simple descriptive statistics of the radiometrically determined uranium and thorium concentrations in the studied unaltered and altered granites of the Wadi Ghadir area

Statistical parameter	Two-mica granite		Altered granite (mineralized granite)	
	U	Th	U	Th
Minimum	6.61	7.95	38.29	5
Maximum	18.52	33.75	225	15
Mean (X)	12.29	19.80	97.95	13.83
S	5.02	8.97	53.37	7.54
C·V(%)	40.85	45.28	53.47	54.5

5 Mineralogical features

Detailed mineralogical examinations for the studied radioactive granites in the shear zone of Wadi Ghadir revealed the presence of primary uranium mineral (uraninite), secondary uranium mineral (uranophane) and accessory minerals such as thorite, monazite, zircon and phlogopite mica. The obtained XRD data for monazite, phlogopite and uranophane are given in Tables 3 and 4 and shown in Fig. 4, respectively. The detailed mineralogical characteristics of the separated heavy minerals showed the following:

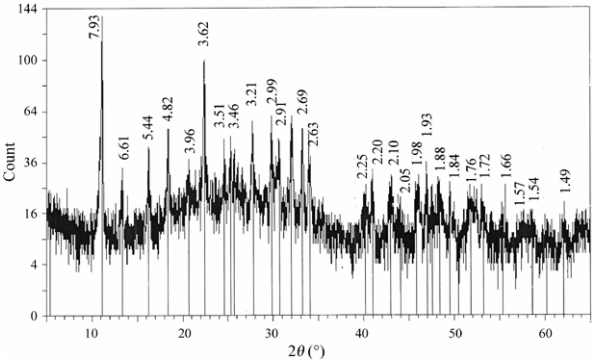

Fig. 4. X-ray diffractogram of uranophane.

Table 3 XRD pattern of monazite

Sample		Monazite ASTM (11-556)	
*d*Å	I/I_0	*d*Å	I/I_0
3.32	46	3.30	50
3.10	100	3.09	100
2.87	52	2.87	70
1.96	66	1.961	25
1.87	29	1.870	18

5.1 Uraninite

Submetallic grayish-black uraninite crystals were detected microscopically and subjected to SEM analysis (Fig. 5A, B). The semiquantitative analysis of uraninite gave U (94.70%), Fe (2.65%), Th (1.36%), Bi (0.98%) and Al (0.32%).

5.2 Uranophane

Under binocular microscope, uranophane grains are found generally as to be massive with a granular form, and their luster is dull and greasy. These grains are distinguished by their bright colors (canary to lemon yellow) with pale yellow streak (Fig. 5C) and present in the forms of fissures and fracture fillings (Fig. 5D). Raslan (2009) identified dark collard iron uraniferous grains in some radioactive granite plutons in the Eastern Desert of Egypt. These grains are composed mainly of uranophane and beta-uranophane coated and stained with limonite. Raslan (2004) remarked that the presence of both uranophane and beta-uranophane as a mixture in some samples is attributed to the presence of both massive granular and fibrous acicular crystals as intergrown mixtures. The SEM data (Fig. 5E, F) confirm the chemical composition of uranophane. The major elements in these crystals are U (72.47%), Ca (8.34%) and Si (5.41%), together with Fe (5.52%), K (3.25%), Al (1.11%), P (0.92%), Th (0.77%), Y (0.72%) and Pb (0.47%).

Table 4 XRD pattern of phlogopite-fluor

Sample		Phlogopite-fluor ASTM (16-352)	
*d*Å	I/I_0	*d*Å	I/I_0
9.97	58	9.96	70
4.99	0.3	5.00	6
3.34	100	3.32	100
2.71	0.2	2.70	2
2.63	1	2.615	20
2.51	13	2.501	10
2.43	0.1	2.428	18
2.18	0.3	2.165	16
2.01	17	1.998	30
1.67	3	1.665	20
1.54	1	1.532	14
1.43	3	1.427	4

5.3 Thorite

Angular to subangular black massive thorite grains were actually detected in the studied bulk samples of radioactive granite in the shear zone of Wadi Ghadir. The obtained ESEM data (Fig. 5G, H) reflect the morphological features of thorite and its semiquantitative chemical composition, respectively. The major elements include Th (45.16%), Si (13.47%), U (7.00%), Ce (4.93%), Y (3.95%), Fe (2.27%) and Pb (3.22%).

5.4 (Ce)-monazite

In peraluminous granites, monazite constitutes a major host for the LREE (except Eu) and the actinides of thorium and uranium (Hinton and Paterson, 1994; Bea, 1996) and it commonly contains a minor amount of yttrium and heavy rare-earth elements (HREE). Translucent reddish- orange crystals of monazite were identified under the binocular microscope. These crystals were found in various forms such as massive, granular, angular to subangular and well crystalline habits (Fig. 6A). The data obtained for some of the separated grains by XRD analysis confirm that all the analyzed grains are almost completely composed of monazite (Table 3). ESEM microphotograph and EDX spectra (Fig. 6B, C, D and E) reflect the morphological features of the investigated monazite. However, the obtained results (Fig. 5C, F) confirm the chemical composition of (Ce)-monazite where the major elements include Ce (27.65%–14.75%), P (16.25%–18.93%), La (13.66%–7.25%), Nd (9.93%–6.44%), Th (12.26%–23.50%) with U (1.23%–3.30%), Y

(3.15%–3.44%), Sm (1.86%–1.50%), Ca (1.15%–5.93%) and Fe (1.48%–0.89%) as trace elements.

It is quite clear that the investigated monazites are characterized by the enrichment of both Ce and Th. Several authors have reported that the concentrations of ThO_2 in monazite from the I- and S-type granites similar to those studied here typically range from 4 wt% to 12 wt% (Cuney et al., 1984; Jefferies, 1985; Friedrich and Cuney, 1989; Montel, 1986; Bea, 1996; Forster, 1998). Typical reported concentrations of Nd_2O_3 in monazite-(Ce) from granitic rocks vary between 8 wt% and 12 wt% and Y in average natural monazite ranges from 0.5 wt% to 2.5 wt% (Forster, 1998). The concentrations of UO_2 in granitic monazites rarely exceed 1 wt% (Cuney and Friedrich, 1987), while granitic pegmatites are the only environmental factor for higher uranium concentrations in monazite (Gramaccioli and Segelstad, 1978). Accordingly, the studied monazite variety most probably falls within the compositional limits of other (Ce)-monazites cited in the previous literature.

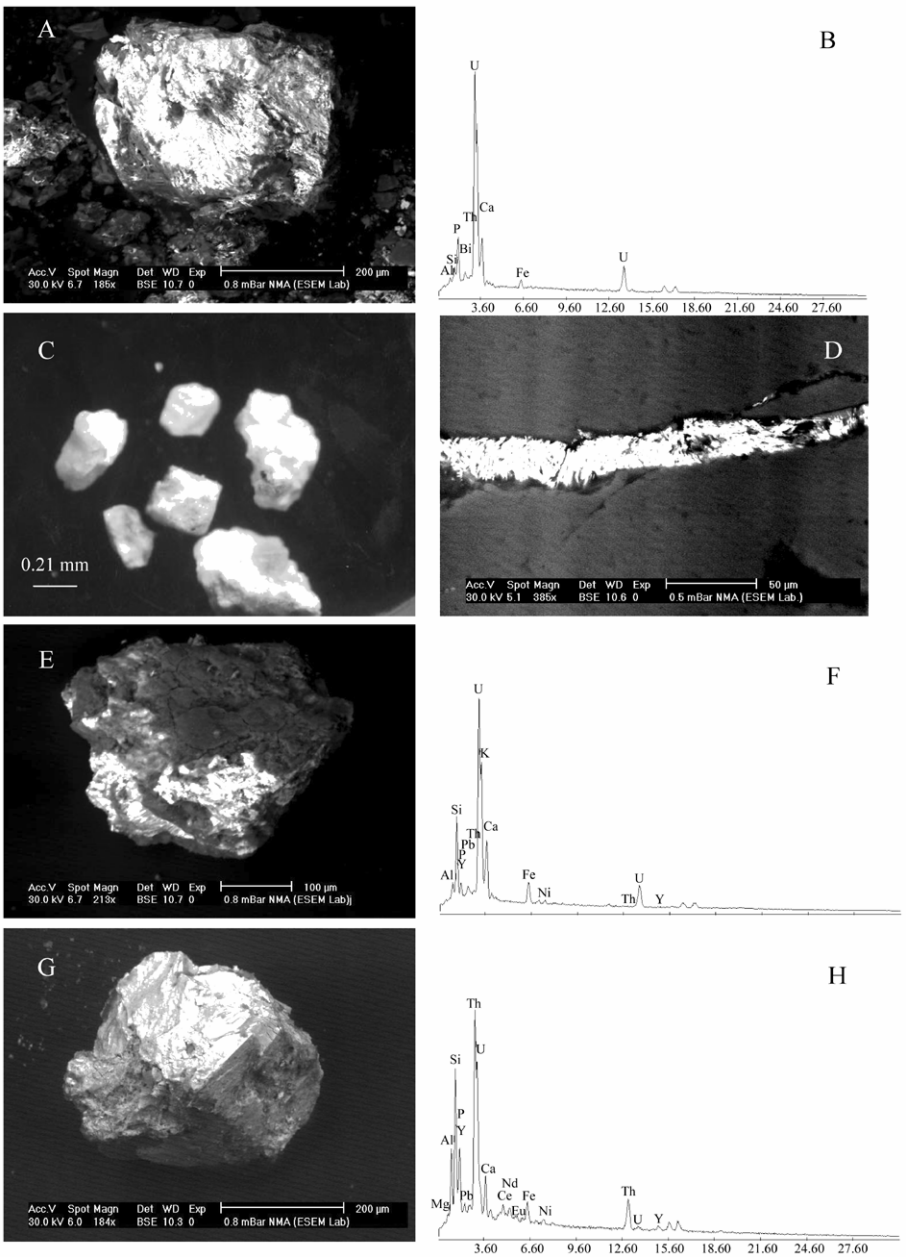

Fig. 5A and B. SEM backscattered images and EDX analyses for the separated uraninite; C. canary to lemon yellow uranophane, binocular microscope; D and E. SEM backscattered images of uranophane in the form of fissures and fracture fillings and as massive granular form, respectively; F. EDX analyses of uranophane; G and H. SEM backscattered images and EDX analyses for the separated thorite.

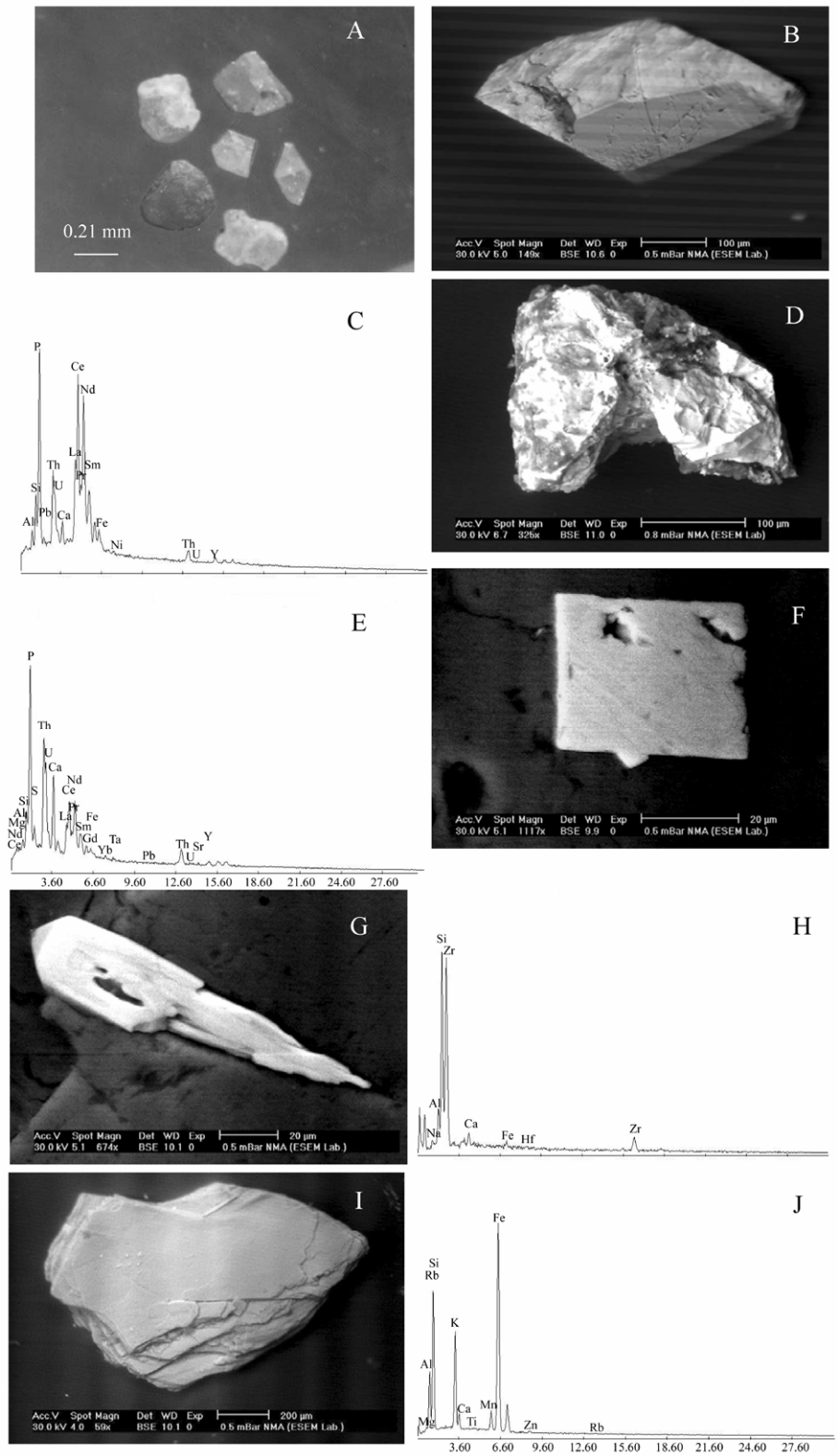

Fig. 6A. Monazite crystals of pale to dark yellow colors, binocular microscope; B, C, D and E. SEM backscattered images and EDX analyses for the various habits of separated monazite; F, G and H. SEM backscattered images and EDX analyses for the various habits of separated zircon; I and J. SEM backscattered images and EDX analyses for the studied mica flakes.

5.5 Zircon

Zircon occurs as pale to dark brown massive compact grains that are generally translucent to opaque. Morphologically, some crystals are typically short to equidimensional, with a length/width ratio of 1:1 and tend to exhibit square to trapezoid, rhombic or hexagonal cross sections. Other euhedral elongated crystals are present and show slight to moderate roundness at one or both ends and terminations of the pyramidal and/or prismal faces, most probably as a result of late magmatic corrosion. The SEM microphotographs (Fig. 6F, G) reflected various morphological features of zircon. The EDAX analysis (Fig. 6H) reflects the chemical composition of zircon. The latter indicates that the major elements in zircon are Zr (50.98%–55.80%) and Si (33.49%–34.11%) with appreciable amounts of Hf (3.02%–3.30%), U (1.23%) and Fe (1.34%).

5.6 Phlogopite

Dark brown to black mica was identified using both XRD and ESEM techniques. The obtained XRD data for picked mica flakes revealed that the studied mica is mainly phlogopite-fluor (Table 4). The obtained ESEM data (Fig. 6I, J) reflect the morphological features of mica and its semiquantitative chemical composition, respectively.

6 Concluding remarks

(1) Quartz-diorite, gneissose granodiorite, two-mica granite and perthite leucogranie are the main rock units cropping out in the study area of the Wadi Ghadir shear zone.

(2) Silicification, hematization and kaolinitization are the most important alteration features associated with uranium mineralization in the sheared altered granites.

(3) From the viewpoint of radioactivity the unaltered and altered two-mica granites are considered as uraniferous granites. The average uranium and thorium contents in the unaltered two-mica granites are 12.29×10^{-6} and 19.81×10^{-6}, respectively, and the average Th/U ratio is 1.62. The altered granites have higher concentrations of U (averaging 97.949) but lower Th and Th/U ratio (13.83 and 0.16, respectively), indicating uranium enrichment. Binary relations of eTh/eU against either eU or eTh and eU with eTh in the studied granites suggest that the distribution of radioactive elements is not only related to magmatic activities, but also due to hydrothermal redistribution of radioelements.

(4) The magmatic U and Th are indicated by the presence of uraninite, thorite, zircon and monazite whereas the evidence of hydrothermal mineralization is the alteration of rock-forming minerals such as feldspar and the formation of secondary minerals such as uranophane and pyrite.

(5) Microscopic, XRD and scanning electron microscopic studies revealed the presence of uraninite, uranophane, thorite, Ce-monazite and zircon, in addition to phlogopite-fluor mica in the studied altered granites of the Wadi Ghadir shear zone.

References

Abu Dief A. (1985) *Geology of Uranium Mineralization in Missikat, Qena-Safaga Road, Eastern Desert, Egypt* [D]. pp.242. M.Sc. Thesis. Assiut University, Egypt (unpublished).

Assaf H.S., Mahdy M.A., and El Afandy A.H. (1997) *Egyptian Younger Granites, an Approach to Define Parameters Favoring Formation of Uranium Deposits* [M]. pp.409–420. 3rd Conference on Geochemistry, Alexandria University.

Assaf H.S., Shalaby M.H., Ibrahim M.E., and Rashed M.A. (1996) *Ground Radiometric Survey, Shalatin-Halaib Area, Southeastern Desert, Egypt* [R]. Internal Report, Nuclear Materials Authority, Egypt (unpublished).

Bea F. (1996) Residence of REE, Y, Th and U in granites and crustal protoliths, implications for the chemistry of crustal melts [J]. *Journal of Petrology*. **37**, 521–552.

Cathelineau M. (1987) U-Th-REE mobility during albitization and quartz dissolution in granitoids: Evidence from southeast French Massif Central [J]. *Bulletin Mineralogie*. **110**, 249–259.

Clark S.P.Jr., Peterman J.E., and Heier K.S. (1966) Abundance of uranium, thorium and potassium. In *Handbook of Physical Contents* (ed. Clark Jr.S.P.) [J]. *Geol. Soc. Am. Mem*. **97** (section 24), 521–541.

Cuney M. and Friedrich M. (1987) Physicochemical and crystal-chemical controls on accessory mineral paragenesis in granitoids: Implications for uranium metallogenesis [J]. *Bulletin Mineralogie*. **110**, 235–247.

Cuney M., Le Fort P., and Wang Z.X. (1984) Uranium and thorium geochemistry and mineralogy in the Manaslu leucogranites (Himalaya, Nepal). In *Geology of Granites and Their Metalogenic Relations* [C]. pp.853–873. University Press, Beijing,

Darnely A.G. (1982) "Hot granite": Some general remarks. In: *Uranium in Granites, Geological Survey of Canada* (ed. Maurice Y.T.) [C]. pp.23–81, 1–10.

El-Feky M.G. (2000) *Geology, Geochemistry and Radioactivity of Wadi Hangaliya Area, South Eastern Desert, Egypt* [D]. pp.300. Ph.D Thesis. Cairo Univ., Egypt.

El-Galy M.M. (1998) *Geology, Radioactivity, Geochemistry and Tectonic Setting of Selected Granitic Rocks, West Gulf of Aqaba, Sinai, Egypt* [D]. pp.324. Ph.D Thesis. Tanta Univ., Egypt.

El-Sharkawy M.A. and El-Bayoumi R.M. (1979) The ophiolites of Wadi Ghadir area, Eastern Desert, Egypt [J]. *Ann. Geol. Survey of Egypt*. **9**, 125–135.

Falkum T. and Rose-Hansen J. (1978) The application of radioelement studies in solving petrological problems of the Precambrian intrusive Homme granite in the Flekkefjord area, South Norway [J]. *Chemical*

Geology. **23**, 73–86.

Friedrich M. and Cuney M. (1989) *Uranium Enrichment Processes in Peraluminous Magmatism* [R]. pp.11–35. In Proceedings of IAEA meeting: Uranium Deposit in Magmatic and Metamorphic Rocks. Salamanca, Spain. IAEA-TC-571/2.

Forster H.J. (1998) The chemical composition of REE-Y-Th-U-rich accessory minerals in peraluminous granites of the Erzgebirge-Fichtelgebire region, Germany, Part I: The monazite-(Ce)-brabantite solid solution series [J]. *American Mineralogist*. **83**, 259–272.

Gramaccioli C.M. and Segalstad T.V. (1978) A uranium- and thorium-rich monazite from a south-alpine pegmatite at Piona, Italy [J]. *American Mineralogist*. **63**, 757–761.

Hinton R.W. and Paterson B.A. (1994) Crystallisation history of granitic magma: Evidence from trace element zoning [J]. *Mineralogical Magazine*. **58A**, 416–417.

Hussein H.A. (1978) *Lecture Course in Nuclear Geology* [Z]. Ain Shams University (unpublished).

Ibrahim I.H. and Ali M.A. (2003) The granitic rocks in Wadi Ghadir area, South Eastern Desert, Egypt and occurrence of a secondary uranium mineral [J]. *Egyptian Journal of Geology*. **47**(2), 671–687.

Ibrahim M.E., Saleh G.M., and Abd El-Naby H.H. (2001) Uranium mineralization in the two mica granite of Gabal Ribdab, South Eastern Desert, Egypt [J]. *Appl. Radiat. Isot*. **55**(6), 123–134.

Ibrahim M.E. (1986) *Geologic and Radiometric Studies on Um Ara Granite Pluton, South East Aswan, Egypt* [D]. M.Sc. Thesis. Mansoura University, Egypt.

Jefferies N.L. (1985) The distribution of the rare earth elements within the Carnmenellis pluton, Cornwall [J]. *Mineralogical Magazine*. **49**, 495–504.

Larsen E.S. and Gottfried D. (1960) Uranium and thorium in selected suites of igneous rocks [J]. *Am. J. Sci*. **258A**, 151–169.

Mahdy A.I. (1998) *Petrological and Geochemical Studies on the Younger Granites and Hammamat Sediments at Gattar-5, Uranium Occurrence, Wadi Balih, North Eastern Desert, Egypt* [D]. pp.185. Ph. D. Thesis. Ain Shams Univ., Egypt.

Matolin M.M. (1991) *"Construction and Use of Spectrometric Calibration Pads", Laboratory of Gamma-ray Spectrometry, N.M.A., Egypt* [R]. A report to the Government of the Arab Republic of Egypt. Project Egy. **4**, 030–03, IAEA.

Montel J.M. (1986) Experimental determination of the solubility of Ce-monazite in SiO_2-Al_2O_3-K_2O-Na_2O meets at 800℃, 2 kbar, under H_2O-saturated conditions [J]. *Geology.* **14**, 659–662.

Raslan M.F. (2004) *On the Distinction Between Uranophane and Beta-uranophane from Some Uraniferous Granitoids in the Eastern Desert of Egypt* [C]. pp.45–52. In Seventh International Conference on the Geology of the Arab World, Cairo University.

Raslan M.F. (2009) Occurrence of uraniferous iron grains at Gabal Gattar, El Missikat and El Erediya granites in Eastern Desert of Egypt [J]. *Resource Geology*. **59**(1), 99–105.

Reeves R.D. and Brooks R.R. (1978) *Trace Element Analyses of Geological Materials* [M]. pp.421. John Wiley & Sons Inc., New York.

Rogers J.J.W. and Adams J.A.S. (1969) Uranium and thorium. In *Handbook of Geochemistry* (ed. Wedepohl K.H.) [C]. VII-3, 92-B-1 to 92-0-8, 90-B-1 to 90-0-5. Springer Verlag, Berlin.

Rogers J.J.W. and Rangland P.C. (1961) Variation of thorium and uranium in selected granitic rocks [J]. *Geochim. et Cosmochim. Acta*. **25**, 99.

Roz M.E. (1994) *Geology and Uranium Mineralization of Gabal Gattar Area, North Eastern Desert, Egypt* [D]. pp.175. M.Sc. Thesis. Al Azhar Univ., Egypt (unpublished).

Sabet A.H., Tosogoev V.B., Bessonenko V.V., Baburin I.M., and Pokryshkin V.I. (1978) Some geological and tectonic peculiarities of the Central Eastern Desert of Egypt [J] *Geol. Surv. Egypt*. **6**, 33–52.

Surour A.A., El-Bayoumi R.M., Attawiya M.Y., and El-Feky M.G. (2001) Geochemistry of wall rock alterations and radioactive mineralization in the vicinity of Hangaliya auriferous shear zone, Eastern Desert, Egypt [J]. *Egyptian Journal of Geology*. **45**(1), 187–212.

Takla M.A., Basta F.F., Shenouda H.H., and El-Maghraby A.M. (1992) Geochemistry of geneisses and granitoids of Wadi Ghadir area, Eastern Desert, Egypt [J]. *GAW.* Cairo Univ. **I**, 477–489.

Whitfield J.M., Rogers J.J.W., and Adams J.A.S. (1959) [J].*Geochimica et Cosmochimica Acta.* **17**, 248–271.

Yanting W., Mingyue F., and Zhuyong S. (1982) *Uranium Geochemistry of the Granites in Eastern Guangdong Province* [C]. pp.637–649. International symposium held at Nanjing.